Obrabotka metallov (tekhnologiya, oborudovanie, instrumenty) = Metal Working and Material Science. 2026 vol. 28 no. 3 pp. 269–285
ISSN: 1994-6309 (print) / 2541-819X (online)
DOI: 10.17212/1994-6309-2026-28.3-269-285

NSTU NETI

Obrabotka metallov -
Metal Working and Material Science

Journal homepage: http://journals.nstu.ru/obrabotka_metallov

Increased hardness and wear resistance of 1.1% C-13% Mn steel after shot peening

Yulia Karlina [1, a, *], *Vladimir Konyukhov* [2, 3, b], *Tatiana Oparina* [2, c]

[1] National Research Moscow State University of Civil Engineering, 26 Yaroslavskoe Shosse, Moscow, 129337, Russian Federation
[2] Irkutsk National Research Technical University, 83 Lermontova str., Irkutsk, 664074, Russian Federation
[3] Cherepovets State University, 5 Lunacharsky pr., Cherepovets, 162600, Russian Federation

[a] https://orcid.org/0000-0001-6519-561X, jul.karlina@gmail.com; [b] https://orcid.org/0000-0001-9137-9404, konyukhov_vyu@mail.ru;
[c] https://orcid.org/0000-0002-9062-6554, martusina2@yandex.ru

ARTICLE INFO

Article history:
Received: 04 June 2026
Revised: 13 June 2026
Accepted: 29 July 2026
Available online: 15 September 2026

Keywords:
Shot peening
Hardness
Phases
Hadfield Steel
Wear and tear
Abrasive
Friction
Hardening
Dislocations
Deformation twins

ABSTRACT

Introduction. Cast high-manganese steel exhibits excellent work hardening and high impact toughness, making it well suited for impact wear applications. Significant wear may occur in the early stages of steel service before sufficient work hardening develops near the surface. To mitigate this initial wear, this study investigates the microstructural characteristics of the hardened layer formed by shot peening and its effect on wear. ***The purpose of this work*** is to investigate the effect of pre-strain induced by shot peening on hardness and abrasive wear. **Materials and methods.** Specimens of *1.1% C-13% Mn* steel were shot peened using a machine with a treatment area of 100% of the specimen surface. A cast steel ball with a nominal diameter of 2 mm was used, and the direction of impact on the specimen surface was set at 85°. The air pressure was 0.35–0.50 MPa, and the treatment duration was in the range of 5–120 min. *Vickers* microhardness was measured using a microhardness tester under an applied load of 0.49 N for 10 s. The morphology of the worn surface was examined using an optical microscope and a scanning electron microscope (*SEM*). The surface wear profile was measured with an optical profilometer. The surface structure of the specimens was examined by X-ray diffraction (*XRD*) with *Cu Kα* radiation using a *Shimadzu XRD-7000* diffractometer. **Results and discussion.** Severe non-uniform plastic deformation was observed at a depth of approximately 60 μm from the surface. It was shown that the surface layers of the shot-peened samples consist of austenite, without any martensitic transformations. To confirm whether stress-induced austenite-to-martensite transformation occurs in the strain-induced twin layers formed by steel shot peening, the subsurface cross-sectional microstructure was analyzed using *EBSD*. The surface hardness of the original *1.1% C-13% Mn* steel specimen increased by a factor of 1.2–2.5 after varying treatment times. An increase in abrasion resistance in wear tests was observed after shot peening. A cutting wear pattern was dominant for the original untreated specimen. However, for the shot-peened specimen, the cutting-mark morphology completely disappeared. Abrasion wear tests showed that higher maximum hardness in the hardened layer corresponds to lower wear loss. These results demonstrated that shot peening effectively improves the wear resistance of high-manganese cast steel by promoting the formation of a hardened surface layer.

For citation: Karlina Yu.I., Konyukhov V.Yu., Oparina T.A. Increased hardness and wear resistance of 1.1% C-13% Mn steel after shot peening. *Obrabotka metallov (tekhnologiya, oborudovanie, instrumenty) = Metal Working and Material Science*, 2026, vol. 28, no. 3, pp. 269–285. DOI: 10.17212/1994-6309-2026-28.3-269-285. (In Russian).

Introduction

Austenitic cast steels with a *Mn* content of 11–14 wt.% (*Hadfield* steel; the Russian equivalent is *110Г13Л* steel) are widely used in aggressive erosive environments involving abrasive wear and impact loading, owing to their non-magnetic properties, excellent toughness, and wear resistance [1–5]. The *Mn* and *C* contents vary depending on the application, with appropriate amounts of alloying elements such as *Cr*, *Mo*, and *V* being added to the composition. The key characteristic of *Hadfield* steels is their exceptional

*** Corresponding author**
Karlina Yulia I., Ph.D. (Engineering), Research Associate
National Research Moscow State Construction University,
26 Yaroslavskoe shosse,
129337, Moscow, Russian Federation
Tel.: +7 914 879-85-05, **e-mail:** jul.karlina@gmail.com

ability to work-harden under deformation while maintaining impact toughness. This is why *Hadfield* steels are ideally suited for applications requiring wear resistance and strain hardening, such as in the mining industry, where they are used as linings for cone crushers that undergo indentation (strain hardening) and abrasive wear. Owing to the increasing demand for extended service life of castings, the development of high-manganese cast steels continues to be an active area of research [5–10].

Typically, castings such as railroad crossings, linings, impellers, blades, and hammer crusher jaws are produced by vacuum forming (*V*-process) and self-hardening in sand molds. These castings must be heat-treated (water-quenched) before use, since eutectic carbides formed at austenite grain boundaries during post-casting cooling reduce impact toughness [10–14]. After heat treatment, the finished cast components are put into service. However, significant wear may occur during the early stages of operation, before sufficient work hardening develops near the surface.

It should be noted that a large body of high-quality scientific literature – including articles and monographs – has been published on austenitic manganese steels, covering their mechanical and microstructural properties [3–14]. The number of publications in this field has increased almost three-fold over the past two decades [15], with a marked rise in recent years, indicating active research efforts by many groups on the development of these steels and their processing methods.

It is well known that high-manganese cast steel undergoes surface hardening during impact loading in service, leading to the formation of a surface-hardened layer. Wear resistance depends on the thickness and maximum hardness of this layer. However, in most high-manganese steel castings, wear and fracture readily occur in the early stages of operation, before full work hardening has taken place. To enhance wear resistance and deformation resistance, considerable efforts have been made to harden the surface of high-manganese steel castings prior to service. Typical surface hardening processes include high-speed impact treatment, explosive hardening, repeated impact hardening, and shot blasting [15–22]. Each of these processes has its advantages and limitations [23–27]. The surface-hardened layers produced by high-speed impact treatment, explosive hardening, and repeated impact treatment are relatively thick; however, these methods require expensive equipment and are not suitable for castings with complex geometries.

Shot blasting is a surface hardening technique that primarily improves surface properties by high-velocity projection of fine particles onto the material surface. The impact energy of the shot particles induces plastic deformation in the surface layer, generating compressive residual stresses [8–12] and enhancing mechanical strength, wear resistance, fatigue strength, and corrosion resistance [18–20, 28–29]. In addition, the impact energy can promote grain refinement and microstructural improvement [28, 29], thereby improving overall material performance. Although numerous macroscopic studies have consistently confirmed that the impact energy during shot blasting has a significant strengthening effect on material properties, the specific mechanism of interaction between the shot particles and the processed surface at the microscopic level remains poorly understood. Similarly, the fundamental principles underlying grain refinement and microstructural changes induced by impact energy are still not fully clarified.

Extensive experimental and simulation studies have been conducted to evaluate various surface hardening methods and to elucidate their mechanisms with regard to the mechanical and fatigue properties of materials. The authors of [19] investigated the effect of shot blasting on the surface characteristics of structural steel. After shot blasting, surface roughness, residual stresses, hardness, and wear resistance were measured, and the influence of processing temperature on surface properties was examined. The results showed that shot blasting significantly improved the wear resistance of the workpiece surface. However, the hardened layer obtained in that study was limited to a thickness of no more than 0.1 mm. Several studies have been published not only on the experimental level but also on the practical application of shot-blasting surface hardening to high-manganese cast steel [5, 6, 19, 24, 25]. To improve surface characteristics, considerable modifications to shot-blasting techniques have been explored, such as stress impact, solid shot blasting, and thermal shot blasting [27, 28]. Nevertheless, there are very few reports on how the microstructure evolves under shot-blasting treatment before and after service operation of machine parts and mechanisms.

The present study examines the effect of shot blasting on the hardness and wear behavior of austenitic high-manganese steel. As noted above, large compressive residual stresses in the surface layer after shot blasting are very effective in increasing the fatigue strength of components. Therefore, shot blasting is widely used to prevent the initiation and propagation of cracks. However, it should be recognized that excessive deformation can itself be a source of fatigue failure [28, 29]. Virtually no open-literature studies are available on this specific aspect.

The purpose of this work is to evaluate the effect of shot-blasting time on the hardness and wear resistance of *1.1% C–13% Mn* steel, addressing ***the following tasks***:

– determination of shot-blasting process parameters to achieve the required hardness values;

– comprehensive characterization of the surface layer after shot blasting using optical and electron microscopy and X-ray phase analysis;

– abrasive wear testing with instrumental assessment of the surface topography of the samples after shot blasting.

Materials and methods

Plates of *1.1% C–13% Mn* steel with dimensions of 100×100 mm and a thickness of 10 mm were selected as the starting material. The chemical composition is shown in Table 1.

Table 1

Chemical composition of *1.1% C-13% Mn* steel castings according to *GOST 977-88*

Element	*C*	*Si*	*Mn*	*Cr*	*Ni*	*Cu*	*S*	*P*
GOST specification, wt.%	0.90–1.50	0.30–1.00	11.50–15.00	≤1.00	≤1.00	≤0.30	≤0.05	≤0.120
Actual content, wt.%	1.12	0.98	12.34	0.60	0.10	0.20	0.05	0.034

The steel samples were subjected to shot blasting using an *S100*-type machine (manufacturer: China) with 100 % coverage of the sample surface. A cast steel ball with a nominal diameter of 2 mm was used as the blasting medium, and the impact angle relative to the sample surface was set to 85°. The air pressure ranged from 0.35 to 0.5 MPa, and the treatment duration varied from 5 to 120 minutes.

Vickers microhardness was measured using an *MX-5* microhardness tester at an applied load of 0.49 N for a dwell time of 10 s. The morphology of the worn surface was examined using a *C-2700* scanning electron microscope (*SEM*). The wear profile in cross-section was assessed using a *Bruker* Contour *GT-K1* optical profilometer equipped with a rotary head; this fully automated, programmable instrument was used to measure the depth of wear grooves and to construct three-dimensional surface maps.

The morphology of the surface layer after shot blasting was examined using a *C-2700 SEM*. Cross-sections of the treated samples were first observed under an optical microscope. The surface structure was studied by X-ray diffraction (*XRD*) using *Cu K***α** radiation in a Shimadzu *XRD-7000* diffractometer. The microstructural features of the surface layer were further characterized by electron backscatter diffraction (*EBSD*). For *EBSD* analysis, the sample surfaces were ground on a Mitsui precision grinding machine (model: *300HMD*) with abundant coolant to minimize thermal effects. The samples were mounted on the magnetic chuck of a rotary surface grinder, and the grinding wheel speed was set to 1,200–1,500 rpm. *EBSD* data were acquired using a *Zeiss Supra 55VP* scanning electron microscope equipped with an *Oxford Symmetry EBSD* camera and an *Oxford X-Max EDS* detector. Data collection was performed using *Oxford AZt*ec software (version 4.2 SP1) at an accelerating voltage of 20 keV and a beam current of 5 nA. After automated diffraction pattern indexing and *EBSD* map acquisition over an 8-h period, the quality of the data sets was evaluated. The average indexing rate for the samples was 84–89 % [20, 21].

Wear resistance tests were conducted in accordance with *GOST 23.208-79* “Conditions for Testing Wear Resistance by Rubbing a Sample Against a Loose Abrasive”. The sample was pressed with a force of 54.1 ± 0.25 N against a rubber roller rotating at a speed of 50 ± 2 rpm, with abrasive particles passing over the sample surface. The reference material was *1.1% C–13% Mn* steel in the as-delivered condition, and grade 12A electrocorundum (according to *GOST 28818-90*) was used as the abrasive. The abrasive wear index was calculated as $\boldsymbol{M} = m_1 - m_2$, where m_1 is the initial mass of the sample and m_2 is the final mass after testing. The samples were weighed on an *Acculab* electronic balance with an accuracy of ±0.0001 g. Each test was performed at least three times. The relative wear resistance ($\boldsymbol{C_i}$) of the test material was calculated according to *GOST 23.208-79* using the following formula:

$$C_i = \frac{\overline{g_{ref}}\rho_{test} N_{test}}{\overline{g_{test}}\rho_{ref} N_{ref}},$$

where g_{ref} and g_{test} are the densities of the reference and test materials, respectively, g/cm^3; N_{ref} and N_{test} are the number of roller revolutions during testing of the reference and test materials, respectively; ρ_{ref} and ρ_{test} are the mass loss of the reference and test samples, respectively, g.

Results and discussion

The investigated *1.1% C–13% Mn* alloy exhibited a single-phase austenitic microstructure with grain sizes ranging from about 100 to 200 μm. Fig. 1 presents an optical microscopy image of the cross-sectional structure of the *Hadfield* steel following 20 min of shot-blasting treatment. Intense plastic deformation is readily discernible down to a depth of approximately 60 μm beneath the top surface. It is evident that the deformation is inhomogeneous.

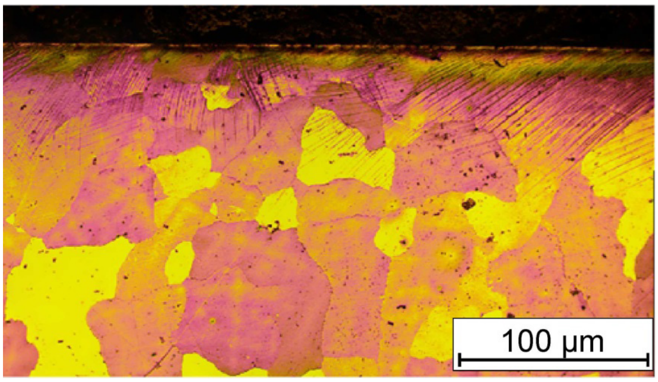

a

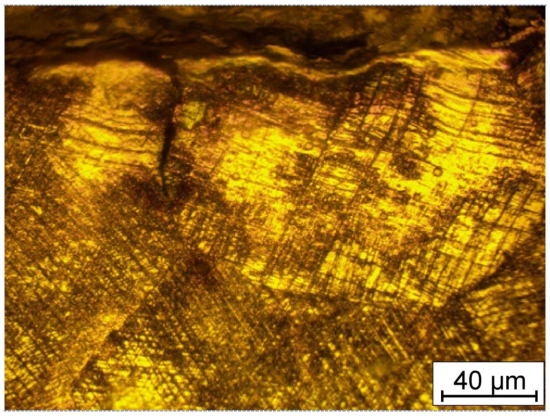

b

Fig. 1. Microstructure of *1.1% C-13% Mn* steel after 20-minute shot peening (optical microscopy): *a* – general view of the surface layer; *b* – hardened layer with traces of deformation twinning

Fig. 2 presents the X-ray diffraction pattern recorded from the treated surface. Five well-defined peaks were detected at 2θ angles of 43.7°, 50.8°, 74.9°, 90.2°, and 96.3°, corresponding to distinct crystallographic planes of the austenitic phase. Apart from a consistent angular shift, the peak positions showed no significant variation among the samples.

Analysis of the X-ray diffraction results showed that with increasing shot-blasting time, all diffraction peaks of the shot-blasted samples shifted significantly toward higher *Bragg* angles. This displacement indicates a continuous increase in plastic deformation and the associated development of residual compressive stresses [24–29]. At the same time, no new diffraction peaks were observed in the patterns of the shot-blasted samples, indicating the absence of martensite, carbide, or other new phase formation during processing.

Fig. 3 shows the surface of the sample under an electron microscope together with an inverse pole figure (*IPF*) color map of the as-received material.

The color variations within the grains qualitatively reflect differences in internal disorientation. *Hadfield* steels have an austenitic (face-centered cubic) structure and a low stacking fault energy (*SFE*) [1, 2, 7, 8, 24–29]. The low *SFE* promotes the formation of deformation twins, while the high concentration of

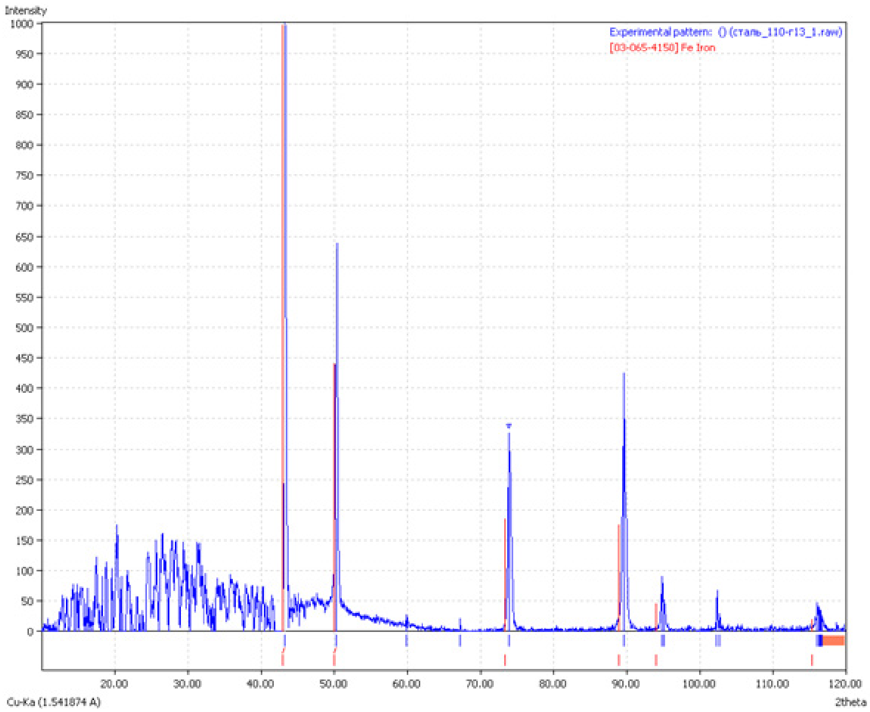

Fig. 2. X-ray diffraction pattern of the surface of *1.1% C-13% Mn* steel

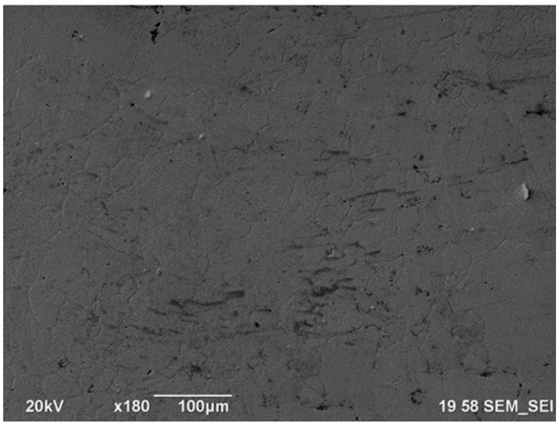

a

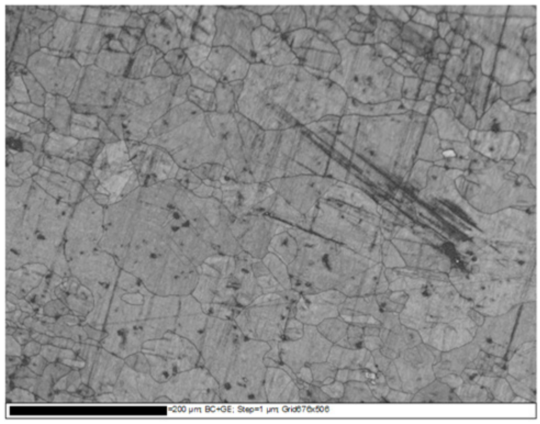

b

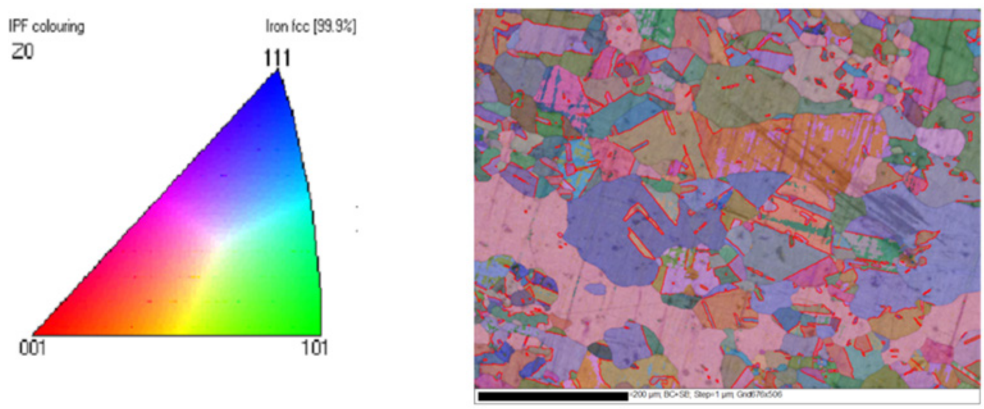

c

Fig. 3. Results of microstructural characterization of the surface layer of *1.1% C-13% Mn* steel after shot peening:

a – *SEM* image of the austenite grain structure in the surface layer; *b* , *c* – *EBSD* inverse pole figure maps interstitial carbon atoms significantly increases the friction stress, which affects the nucleation stress for twinning. During deformation, continuous nucleation and growth of twins occur [3, 15], leading to a sustained strengthening effect via the dynamic *Hall–Petch* mechanism and a high strain-hardening rate, thus imparting excellent strength and ductility to the alloy.

During shot blasting, metallic balls repeatedly impact the surface at high velocity, generating high-density dislocations and deformation twins. On the one hand, the dislocations produced can rearrange under stress to form dislocation networks, which leads to the formation of nanocrystallites separated by blurred grain boundaries [24, 25]. On the other hand, deformation twins effectively subdivide the original grains by introducing new boundaries, resulting in a refined microstructure. Some studies, based on transmission electron microscopy observations, have reported the formation of a nanocrystalline structure with random orientation in the surface layer of *Hadfield* steel [24–26]. According to the authors of [24], the formation of nanocrystallites can be attributed to several factors: very large deformation, extremely high strain rates, and cyclic loading during shot blasting. The substantially increased strain and strain rate activate a high density of dislocations and multiple-system deformation twins to accommodate the applied stress [22–25].

Fig. 3,*b*, *c* shows inverse pole figure (*IPF*) maps obtained from the *EBSD* analysis of the investigated samples. The sample without shot blasting shows no significant deformation bands (Fig. 3,*a*). After 5–15 min of shot blasting (Fig. 3,*b*), deformation bands formed within the grains. As the processing time increased, these bands became increasingly dense, indicating progressive accumulation of plastic deformation from repeated impacts, which gradually subdivided the original grains. When the shot-blasting duration was extended to 40 min, the density of deformation bands reached a maximum, which subsequently led to grain fragmentation. The random crystallographic orientation of these newly formed grains is reflected in a more dispersed and chaotic color distribution on the map in Fig. 3,*c*. After 60 min of shot blasting, the color distribution showed no significant further changes, indicating stabilization of the grain fragmentation process and saturation of the deformation band density.

The measured average grain size as a function of shot-blasting duration is consistent with the microstructural observations. The grain size decreased from 100 μm (0 min) to 62 μm (40 min) and finally to 57 μm (60 min). These data confirm that shot blasting effectively refines the **γ**-*Fe* grains.

Analysis of low-angle grain boundary (*LAGB*) maps (misorientation angles <15°) of samples subjected to shot blasting for various durations revealed a significant proportion of *LAGBs* in all conditions. The quantitative data presented in Table 2 show a marked increase in the *LAGB* fraction after shot blasting. In particular, this fraction increased from 27.4 % in the untreated sample to over 70 % in all shot-blasted samples, confirming the high density of *LAGBs* generated by the process. It is noteworthy that a value of 69.2 % was achieved after only 5 min of treatment. These results indicate that shot blasting generates a large number of dislocations. During plastic deformation, these dislocations become tangled, and their motion is hindered by obstacles such as grain boundaries and twin boundaries, leading to the formation of dislocation clusters. The subsequent accumulation and reorganization of these dislocations result in the formation of the observed low-angle grain boundaries.

Table 2

Change in the fraction of low-angle grain boundaries in the studied steel with different shot peening durations

Shot peening time (min)	0	5	10	15	40	60
Low-angle grain boundary fraction *LAGB* (%)	27.4	69.2	74.5	79.9	79.3	74.3

Fig. 4 presents the hardness profiles as a function of depth (Fig. 4,*a*) and as a function of shot-blasting duration (Fig. 4,*b*). The surface hardness was substantially increased by shot blasting, rising from 300 HV in the untreated state to 743 HV after 30 min of treatment. Extending the processing time to 60 min produced a modest further increase to 774–785 HV. These peak hardness values are close to the maximum hardness attainable in high-manganese steel via surface impact hardening, as documented in previous studies [10, 16, 17, 24].

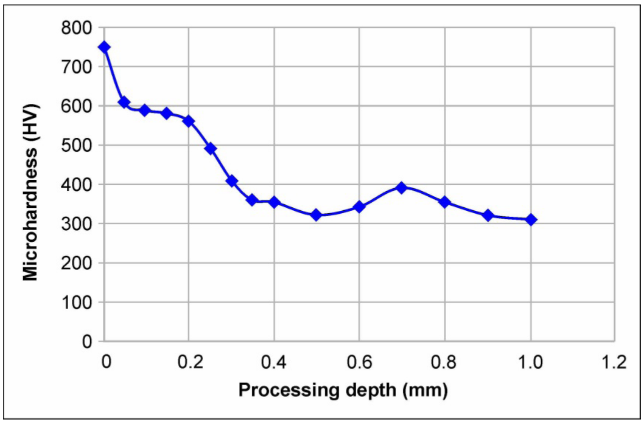

a

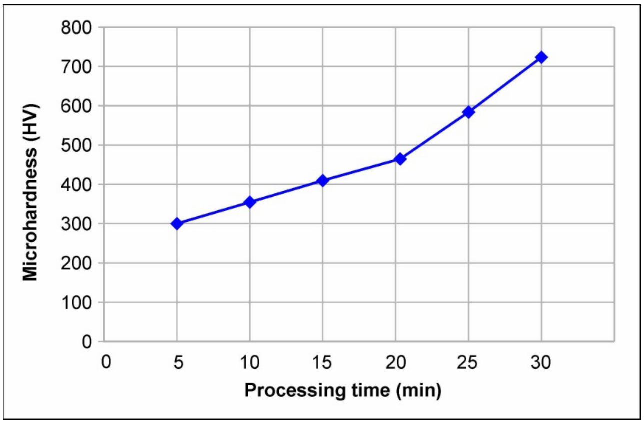

b

Fig. 4. Microhardness values of the surface layer of *1.1% C-13% Mn* steel after shot peening:

a – depth-dependent hardness distribution from the surface after 15-minute shot peening; *b* – variation of surface layer hardness with shot peening duration

For all shot-blasted samples, hardness gradually decreased with increasing distance from the surface, eventually approaching the level of the untreated sample. A slight increase in hardness at a depth of 0.7–0.8 mm (see Fig. 4,*a*) does not affect the general trend of decreasing hardness from the surface through the depth of the hardened layer and is most likely associated with features of the metallurgical process.

The thickness of the hardened layer, defined as the depth at which the hardness was at least 450–500 HV, was 20, 170, 310, 480, and 600 μm for samples treated for 5, 10, 15, 40, and 60 min, respectively. It is noteworthy that the hardness gradient became less pronounced with increasing shot-blasting time. Overall, the results confirm that shot blasting successfully created a hardened layer on the surface of the high-manganese steel, and that the layer depth increases with processing time; however, the depth increase is naturally not linear, even at 60 min. The formation of this hardened layer is crucial for enhancing the wear resistance of the material.

Our results surpass those reported in [19] in terms of both hardness and hardening depth. In that study, after shot blasting, the hardness at a depth of 0.03 mm reached a maximum of 600 HV when using hardened steel shot and 580 HV when using low-carbon steel shot. However, at a depth of 0.1 mm from the surface, the hardness dropped to 220 HV, which is similar to the untreated sample.

The results of the abrasive wear tests are shown in Fig. 5. The mass loss of the steel in the as-cast state and after shot blasting, as a function of test duration, is presented in Fig. 5. It can be seen from the figure that mass loss increases with test time for all conditions. The difference between the samples lies in the rate of mass loss. The untreated sample exhibited higher mass loss under all conditions. Samples subjected to shot blasting for 15 min and above showed low mass loss values. The relative wear resistance of *1.1% C–13% Mn* steel after shot blasting is presented in Table 3.

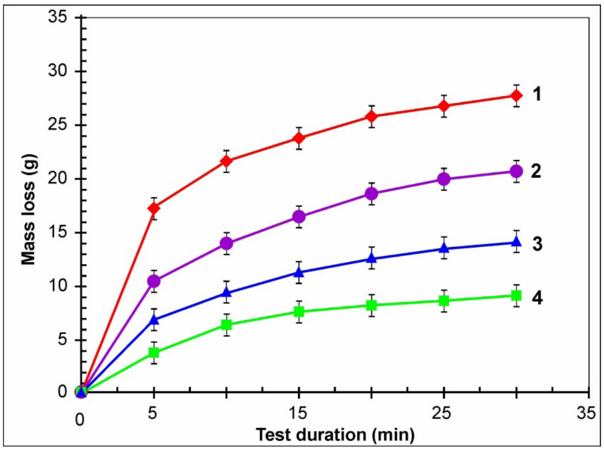

Fig. 5. Results of abrasive wear tests as a function of test duration:

1 – untreated sample; 2 – shot-peened for 15 min; 3 – shot-peened for 30 min; 4 – shot-peened for 60 min)

Table 3

Relative wear resistance of *1.1% C-13% Mn* steel after shot peening

No.	Specimen / treatment	m_0–m_1	m_1–m_2	m_2–m_3	m_3–m_4	m_4–m_5	Overall wear (g)	Relative wear resistance compared to *1.1% C-13% Mn steel*
1	*1.1% C-13% Mn* steel, untreated	1.0714	0.3525	00.2588	0.2202	0.1465	22.0494	1.0000
2	*1.1% C-13% Mn* steel, treated for 5 min	0.4945	0.2179	0.1567	0.1546	0.1456	1.1693	1.7527
3	*1.1% C-13% Mn* steel, treated for 10 min	0.4829	0.2050	0.1602	0.1435	00.1216	1.1132	1.8410
4	*1.1% C-13% Mn* steel, treated for 15 min	0.7196	0.1452	0.0827	0.0612	0.0520	11.0607	1.9321
5	*1.1% C-13% Mn* steel, treated for 30 min	0.5284	0.2143	0.0961	0.1086	0.0646	1.0120	2.0251
6	*1.1% C-13% Mn* steel, treated for 40 min	0.5884	0.2043	0.0734	0.1016	0.0921	0.9112	2.2494
7	*1.1% C-13% Mn* steel, treated for 60 min	0.3929	0.1218	0.1233	0.1029	0.1002	00.8411	2.4368

Fig. 6 shows *SEM* images of wear scars obtained after friction testing. The worn surface of the untreated sample (Fig. 6,*a*) is covered with deep grooves and light irregular particles or spots. These features are likely wear debris, such as delamination particles, transferred material, or oxides formed due to frictional heating. This morphology suggests that local adhesion and subsequent detachment occurred during sliding. Significant abrasive wear is also evident. Thus, the main wear mechanism for the untreated sample is considered to be adhesive wear, accompanied by substantial abrasive and fatigue wear.

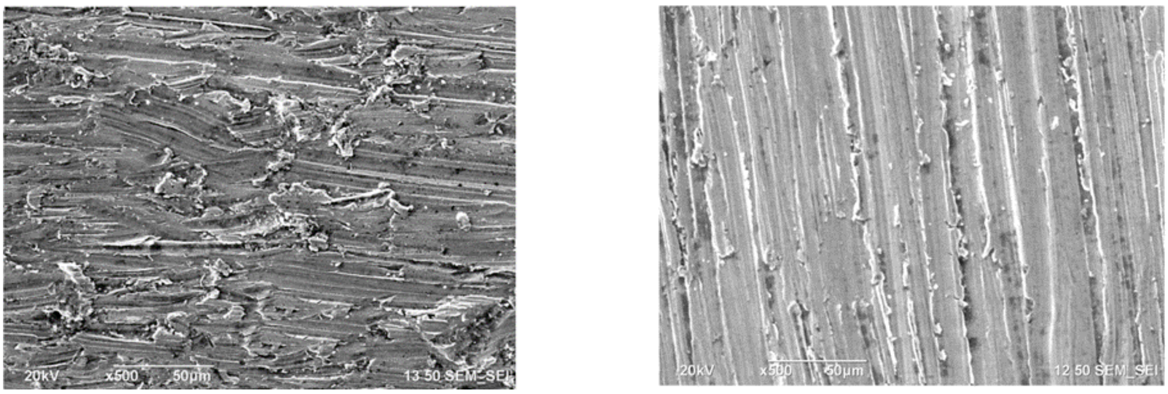

a *b*

Fig. 6. SEM topography of the worn surfaces:

a – untreated; *б* – after 30-min shot peening treatment

In contrast, the shot-blasted samples exhibited regular rectangular (or nearly rectangular) wear marks. Their worn surfaces were relatively smooth, with minor scratches and few wear particles, indicating that abrasive wear is the dominant mechanism with minimal adhesive contribution.

This transition from adhesive to abrasive wear as the dominant mechanism demonstrates how shot blasting changes the wear behavior of high-manganese steel. The increased surface hardness achieved through shot blasting impedes plastic deformation of surface asperities, leading to a pronounced “plowing effect” during abrasive wear.

Fig. 7 shows three-dimensional general morphology of wear scars observed on all tested samples. It is clearly seen that the width of the wear scar on the untreated sample is significantly larger than on the shot-blasted samples. The surface profile is characterized by pronounced peaks and troughs. This is attributed to the rapid increase in surface hardness after shot blasting, which hinders surface plasticization. However, quantitative parameters such as wear depth cannot be obtained directly from these initial morphological images. For quantitative comparison, the three-dimensional morphology data were aligned using the intact area of each sample as a reference plane. A comparative analysis of the wear scars is shown in Fig. 7,*b* and Fig. 8,*b*. Fig. 7,*a* shows the wear profiles of the tested samples. It can be seen that the untreated sample exhibits the greatest wear depth and its wear scar width is significantly greater than that of the shot-blasted samples. This result is consistent with the data in Fig. 8,*a*. For shot-blasted samples, the maximum wear depth gradually decreased with increasing shot-blasting time, reached a minimum at 40 min, and then increased again. The maximum wear scar depth and volume loss (i.e., mass loss) show an almost identical trend, with the exception of the maximum wear depth of the untreated sample. Although the untreated sample has the greatest depth, it also exhibits the greatest volume loss due to the greater width of the wear scar. However, after shot blasting, the surface hardness increases significantly, and volume loss gradually decreases with increasing shot-blasting time. At 40 min, volume loss reached a minimum, and then increased again. Thus, in our tests, the sample demonstrated optimal wear resistance at a shot-blasting time of 40 min. The observed increase in wear at longer times requires additional investigation, which will be addressed in future work.

The results of our research, together with an analysis of the work of other authors [20–25], show that intense, repetitive impacts of steel shot smooth surface irregularities, thereby rapidly reducing surface

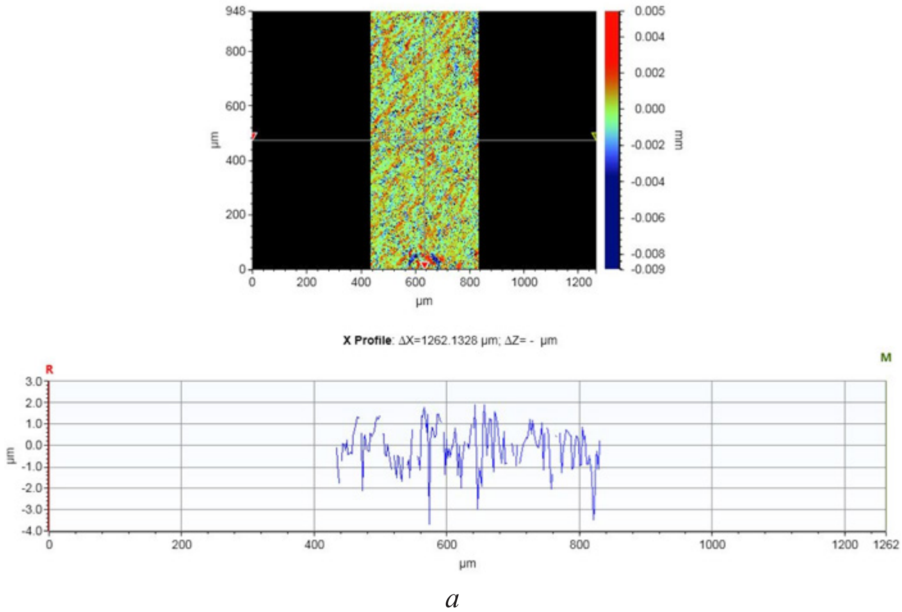

a

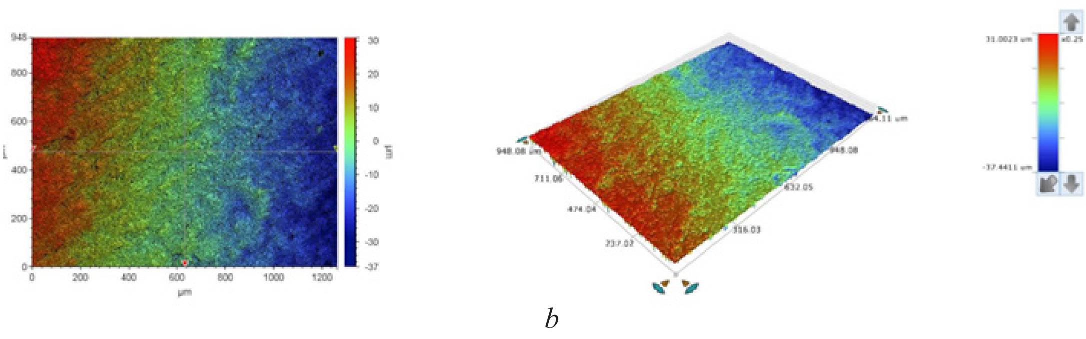

b

Fig. 7. Topography of the worn surface measured by optical profilometry (untreated specimens):

a – surface profile; *b* – height variation of surface irregularities

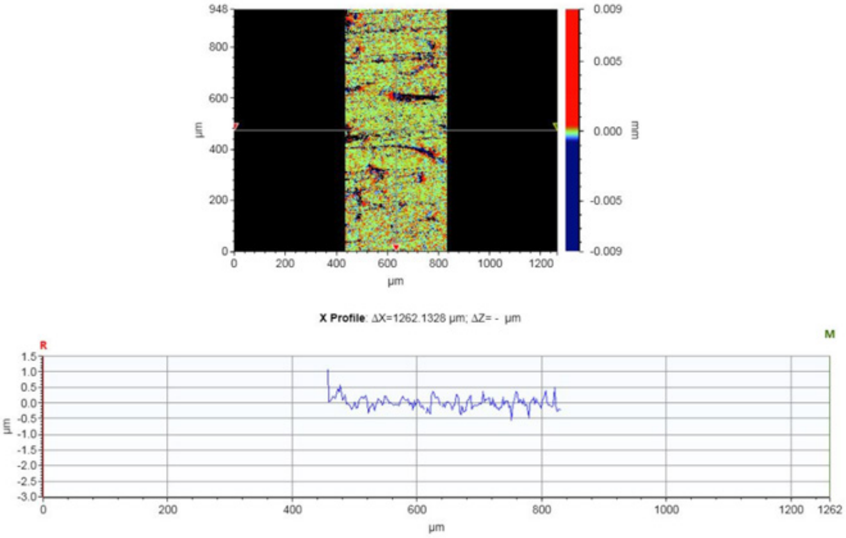

a

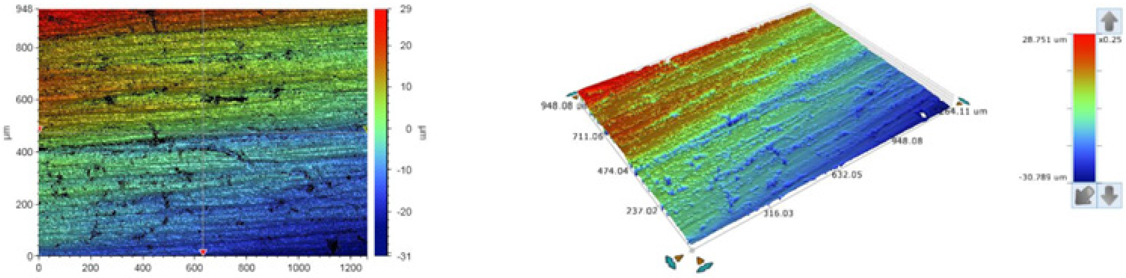

b

Fig. 8. Topography of the worn surface measured by optical profilometry (after shot peening treatment):

a – surface profile; *b* – height variation of surface irregularities

roughness (Fig. 8). At the same time, these impacts create numerous dimples that introduce residual compressive stresses and cause severe plastic deformation. Plastic deformation promotes extensive generation and multiplication of dislocations, leading to a rapid increase in dislocation density. The resulting dislocations interact to form complex configurations (e.g., dislocation walls and cells), and their motion is hindered by microstructural barriers, resulting in clusters and the subsequent formation of subgrain boundaries [4, 7, 10, 27]. This microstructural evolution is accompanied by significant hardening of the surface layer (Fig. 1), which directly increases surface hardness (Fig. 4). During prolonged shot blasting, the grains are refined and the hardened layer thickens. However, as noted by the authors of [12, 14, 17, 20, 21], excessive treatment leads to negative consequences such as microcracks and surface delamination, indicating the onset of surface damage. Consequently, the wear resistance of high-manganese steel first increases and then decreases with increasing processing time, while impact toughness shows a more complex, non-monotonic trend [15–19]. These changes in mechanical properties are explained by the competition between beneficial factors (dislocation hardening, grain refinement, and residual compressive stress) and detrimental factors (surface roughness and microcracks) induced by mechanical impacts.

In conclusion, we note that in this work we studied the effect of shot-blasting duration on the microstructure and properties of *1.1% C–13% Mn* high-manganese steel. The results show that intense, repeated impacts not only improve surface quality but also introduce residual compressive stresses [1–3] and generate a high dislocation density [24, 25]. The entanglement and immobilization of these dislocations at microstructural barriers (e.g., grain boundaries and twins) lead to the formation of dislocation clusters [26, 27], which subsequently transform into low-angle grain boundaries. The microstructure refinement process, driven by sustained plastic deformation, leads to gradual grain refinement with increasing shot-blasting time. As a result, the hardened surface layer thickens, leading to changes in mechanical properties. Both surface hardness and wear resistance show a tendency to initially increase and then decrease, with optimal wear resistance achieved after 40 min of shot blasting. Accordingly, the dominant wear mechanism shifts from adhesive to abrasive wear. This study provides theoretical data and technical support for the use of shot blasting to extend the service life of high-manganese steel components in mechanical engineering. Shot-blasted *1.1% C–13% Mn* steel can certainly improve wear resistance under abrasive wear conditions, which is consistent with the results of other authors [1, 4, 10, 12–14]. It also becomes necessary to reconsider the notion of the insignificance of the effect of surface hardening (work hardening) on the wear resistance of the material. For commercial applications, shot blasting is a suitable process for strengthening metallic materials to increase wear resistance, as an alternative to alloying or other processes that alter the bulk microstructure of materials, especially under low-impact-energy wear conditions.

Conclusions

1. It is found that all *1.1% C–13% Mn* steel samples consist of austenite, with no martensitic transformations occurring in the surface layer during shot blasting. The broadening of the *Bragg* diffraction peaks in the shot-blasted samples can be attributed to grain refinement and/or an increase in lattice strain at the atomic level.

2. It is shown that the surface hardness of the *1.1% C–13% Mn* steel samples increases significantly from 300 HV to 743 HV as the processing time is extended from 5 to 30 min. A further increase in processing time from 30 to 60 min results in a slight additional hardness rise to 774–785 HV. The hardness depth profiles were recorded for shot-blasting durations of up to 60 min. Longer processing times do not lead to further hardness increase.

3. It is found that the relative wear resistance increased by a factor of 1.75–2.44 for treatment durations ranging from 5 to 60 min. To optimize wear resistance, a blasting time of 40 min is recommended, whereas for applications requiring higher impact toughness, a shorter blasting time of 5 min is advisable.

References

1. Xu X., Xu W., Ederveen F.H., Zwaag S. van der. Design of low hardness abrasion resistant steels. *Wear*, 2013, vol. 301 (1–2), pp. 89–93. DOI: 10.1016/j.wear.2013.01.002.

2. Andreev E.E., Tikhonov O.N. *Droblenie, izmel'chenie i podgotovka syr'ya k obogashcheniyu* [Crushing, grinding and preparation of raw materials for beneficiation]. St. Petersburg, SPbGI Publ., 2007. 439 p.

3. Karlina Yu.I., Konyukhov V.Yu., Oparina T.A. Issledovanie abrazivnoi iznosostoikosti poroshkovykh provolok pri naplavke na vysokomargantsovistuyu stal' Gadfil'da [Study of abrasive wear resistance of flux-cored wires during surfacing on high-manganese Hadfield steel]. *Obrabotka metallov (tekhnologiya, oborudovanie, instrumenty) = Metal Working and Material Science*, 2025, vol. 27, no. 4, pp. 287–308. DOI: 10.17212/1994-6309-2025-27.4-287-308.

4. Kolokoltsev V.M., Vdovin K.N., Chernov V.P., Feoktistov N.A., Gorlenko D.A., Dubrovin V.K. Issledovanie mekhanizmov abrazivnogo i udarno-abrazivnogo iznashivaniya vysokomargantsevoi stali [Study of abrasive and impact and abrasive wear mechanisms of high manganese steel]. *Vestnik MGTU im. G.I. Nosova = Vestnik of Nosov Magnitogorsk State Technical University*, 2017, vol. 15, no. 2, pp. 54–62. DOI: 10.18503/1995-2732-2017-15-2-54-62.

5. Chen H., Zhao D., Wang Q., Qiang Y., Qi J. Effects of impact energy on the wear resistance and work hardening mechanism of medium manganese austenitic steel. *Friction*, 2017, vol. 5 (4), pp. 447–454. DOI: 10.1007/s40544-017-0158-6.

6. Xu L.L., Zheng Z.B., Yang H.K., Xu Z.B., Long J., Wang S., Zhao S.Y., Wang H.Y. Adapting medium manganese steels for different wear conditions: insights from aluminum modification. *Journal of Iron and Steel Research International*, 2025, vol. 32, pp. 3504–3519. DOI: 10.1007/s42243-025-01516-2.

7. Chorshanbiev Sh.M., Karimov K.A., Adilova Sh.R., Turakhodzhaev N.D., Erkindzhonov A., Mirmukhamedov M.M., Sharipov J.Kh., Obidov Z.R., Komolov H. Razrabotka iznosostoikikh detalei iz vysokomargantsevoi modifitsirovannoi stali 110G13L [Development of wear-resistant parts from high-manganese modified 110G13L

brand steel]. *Zhurnal Sibirskogo federal'nogo universiteta. Tekhnika i tekhnologii = Journal of Siberian Federal University. Engineering and Technology*, 2024, vol. 17 (2), pp. 175–185.

8. Nezami E.G., Hashash Y.M., Zhao D., Ghaboussi J. Simulation of front end loader bucket–soil interaction using discrete element method. *International Journal for Numerical and Analytical Methods in Geomechanics*, 2007, vol. 31 (9), pp. 1147–1162. DOI: 10.1002/nag.594.

9. Dong Z., Jiang F., Tan Y., Wang F., Ma R., Liu J. Review of the modeling methods of bucket tooth wear for construction machinery. *Lubricants*, 2023, vol. 11, p. 253. DOI: 10.3390/lubricants11060253.

10. Vdovin K.N., Feoktistov N.A., Khabibullin Sh.M. Issledovanie protsessa ekspluatatsii litykh bronei iz stali marki 110G13L v mel'nitse MPSI – 70x23 [Study of the operation process of cast armor plates made of steel grade 110G13L in the MPSI–70x23 mill]. *Liteinye protsessy = Foundry processes*, 2013, no. 12, pp. 8–11.

11. Sinitsyn N.I., Chikova O.A., Chezganov D.S. Vliyanie razrusheniya mikrogeterogennosti na mikrostrukturu i kristallicheskoe stroenie slitkov stali 110G13L (Stali Gadfil'da) [Effect of destruction of microheterogeneity on microstructure and crystal structure of 110g13l steel ingots (Hadfield steel)]. *Chernye metally = Stahl und Eisen*, 2020, no. 1, pp. 36–42. (In Russian).

12. Kwok T.W.J., Dye D. A review of the processing, microstructure and property relationships in medium Mn steels. *International Materials Reviews*, 2023, vol. 68 (8), pp. 1098–1134. DOI: 10.1080/09506608.2023.2199617.

13. Mulyavko N.M. Analiz ekspluatatsionnoi stoikosti otlivok iz stali 110G13L [Analysis of the operational durability of 110G13L steel castings]. *Izvestiya Chelyabinskogo nauchnogo tsentra UrO RAN*, 2001, no. 4, pp. 28–30. (In Russian).

14. Mohapatra S., Satpathy B., Sarkar A., Kumar S., Aich S., Oh M.S. Recent advances in medium-manganese steel: a review of key findings, challenges, and future perspectives. *Journal of Materials Science*, 2025, vol. 60 (23), pp. 9447–9528. DOI: 10.1007/s10853-025-11010-5.

15. Park G., Jeong S., Lee C. Fusion weldabilities of advanced high manganese steels: a review. *Metals and Materials International*, 2021, vol. 27 (7), pp. 2046–2058. DOI: 10.1007/s12540-020-00706-9.

16. Allende-Seco R., Artigas A., Bruna H., Carvajal L., Monsalve A., Sklate-Boja M.F. Hardening by transformation and cold working in a Hadfield steel cone crusher liner. *Metals*, 2021, vol. 11, p. 961. DOI: 10.3390/met11060961.

17. Yan W., Fang L., Sun K., Xu Y. Effect of surface work hardening on wear behavior of Hadfield steel. *Materials Science and Engineering: A*, 2007, vol. 460–461, pp. 542–549. DOI: 10.1016/j.msea.2007.02.094.

18. Balanovsky A.E., Guseva E.A., Konstantinova M.V., Karlina Yu.I. Utochnenie mekhanizma fazovykh i strukturnykh prevrashchenii v stali 110G13L v intervale temperatur nagreva obraztsov pod zakalku ot 920 °S do 1100 °S [Clarification of the mechanism of phase and structural transformations in 110G13L steel in the range of heating temperatures of samples for hardening from 920 °C to 1100 °C]. *Chernye metally = Stahl und Eisen*, 2023, no. 8, pp. 18–25. DOI: 10.17580/chm.2023.08.03. (In Russian).

19. Ngo H.K.L., Okuyama T., Yamamoto K., Nakayama M., Kudo M., Mizuno K., Yagi Y. Microstructure and wear behavior of high-mn austenitic cast steel hardened by air blast shot-peening. *International Journal of Metalcasting*, 2025, vol. 20, pp. 1837–1850. DOI: 10.1007/s40962-025-01699-0.

20. Varyukhin V.N., Pashinskaya E.G., Zavdoveev A.V., Burkhovetskii V.V. *Vozmozhnosti metoda difraktsii obratno-rasseyannykh elektronov dlya analiza struktury deformirovannykh materialov* [Possibilities of the Electron Backscatter Diffraction Method for Analysis of the Structure of Deformed Materials]. Kyiv, Naukova Dumka Publ., 2014. 102 p. DOI: 10.13140/2.1.5016.6720.

21. Doddapaneni S., Kumar S., Sharma S., Shankar G., Shettar M., Kumar N., Aroor G. Advancements in EBSD techniques: a comprehensive review on characterization of composites and metals, sample preparation, and operational parameters. *Journal of Composites Science*, 2025, vol. 9 (3), p. 132. DOI: 10.3390/jcs9030132.

22. Harada Y., Fukaura K., Haga S. Influence of microshot peening on surface layer characteristics of structural steel. *Journal of Materials Processing Technology*, 2007, vol. 191 (1–3), pp. 297–301. DOI: 10.1016/j.jmatprotec.2007.03.026.

23. Bagherifard S., Fernandez-Pariente I., Ghelichi R., Guagliano M. Fatigue behavior of notched steel specimens with nanocrystallized surface obtained by severe shot peening. *Materials & Design*, 2013, vol. 45, pp. 497–503. DOI: 10.1016/j.matdes.2012.09.025.

24. Yan W., Fang L., Zheng Z., Sun K., Xu Y. Effect of surface nanocrystallization on abrasive wear properties in Hadfield steel. *Tribology International*, 2009, vol. 42 (5), pp. 634–641. DOI: 10.1016/j.triboint.2008.08.012.

25. John M., Kalvala P.R., Misra M., Menezes P.L. Peening techniques for surface modification: processes, properties, and applications. *Materials*, 2021, vol. 14 (14), p. 3841. DOI: 10.3390/ma14143841.

26. Świetlicki A., Szala M., Walczak M. Effects of shot peening and cavitation peening on properties of surface layer of metallic materials – A short review. *Materials*, 2022, vol. 15, p. 2476. DOI: 10.3390/ma15072476.

27. Yang G., Kim J.-K. An overview of high yield strength twinning-induced plasticity steels. *Metals*, 2021, vol. 11, p. 124. DOI: 10.3390/met11010124.

Conflicts of Interest

The authors declare no conflict of interest.